Biosensors and Bioelectronics 25 (2010) 1277–1282

Contents lists available at ScienceDirect

Biosensors and Bioelectronics

journal homepage: www.elsevier.com/locate/bios

High-performance glucose amperometric biosensor based on magnetic polymeric bionanocomposites

Can Zou, Yingchun Fu, Qingji Xie*, Shouzhuo Yao

Key Laboratory of Chemical Biology and Traditional Chinese Medicine Research (Ministry of Education of China), College of Chemistry and Chemical Engineering, Hunan Normal University, Changsha 410081, China

ARTICLE INFO

Article history:
Received 17 July 2009
Received in revised form 8 October 2009
Accepted 12 October 2009
Available online 21 October 2009

Keywords:
Magnetic polymeric bionanocomposites
Magnetic immobilization of enzyme
1,6-Hexanedithiol
Glucose oxidase
Amperometric biosensing

ABSTRACT

One-pot chemical oxidation of 1,6-hexanedithiol (HDT) in its aqueous suspension containing glucose oxidase (GOx) and Fe_3O_4–Au nanocomposites by 1,4-benzoquinone yields novel Fe_3O_4–Au–poly(HDT) (PHDT)–GOx magnetic polymeric bionanocomposites (MPBNCs) with GOx immobilized at high load and high activity. Transmission/scanning electron microscopy and UV–vis spectrophotometry are used to characterize the prepared MPBNCs. A Fe_3O_4–Au–PHDT–GOx/Au electrode has been prepared by facile and efficient magnetism separation/immobilization of the MPBNCs onto an Au magnetism-electrode for biosensing of glucose, which exhibits high detection sensitivity (110 $\mu A\,cm^{-2}\,mM^{-1}$), low detection limit (0.33 μM, S/N = 3), rapid response time (<5 s), and excellent anti-interferent ability and stability. The biosensor performs better than those based on the existing protocols of conventional electropolymerization and chemical preoxidation/electropolymerization of monomer. The chemical oxidation synthesis and magnetism separation/immobilization protocol proposed here for convenient preparation and surface immobilization of functional MPBNCs of the target biomolecules may have application potential in many fields, such as biosensing, biocatalysis, biofuel cells, and bioaffinity separation.

1. Introduction

Magnetic nanoparticles are of current interest in bio-applications, e.g. biocatalysis (Wei and Wang, 2008; Yang et al., 2004), bio-labeling (Morais et al., 2004; Schoepf et al., 1998; Tang et al., 2008), and separation/purification of biomolecules (Altintas et al., 2007; Gu et al., 2006; Krizova et al., 2005; Olsvik et al., 1994; Yang et al., 2004). The polymeric nanocomposites (PNCs) with hybrid properties of the involved nanomaterial and polymer have recently attracted extensive research interest in the fields of catalysis (Granot et al., 2005; O'Mullane et al., 2004), electronics (Dang et al., 2008; Shen et al., 2007), and optics (Cao et al., 2007; Ventura and Gu, 2008). Also, the magnetic polymeric nanocomposites (MPNCs) with magnetic nanoparticles embedded possess additional magnetic property for many important applications (Burke et al., 2002; Chung et al., 2007; Liu et al., 2008a,b; Wei et al., 2006; Zhang et al., 2008). Immobilization of biomolecules on/in the MPNCs to yield magnetic polymeric bionanocomposites (MPBNCs) is interesting and important for biosensing and bioseparation (Bayramoglu et al., 2008; Hong et al., 2008; Huang et al., 2007, 2008; Lei et al., 2009). However, the existing researches mainly deal with multi-step synthesis of MPBNCs, probably because the synthesis conditions of the MPNCs precursors are generally rigorous and not favorable for retaining the bioactivity of the target biomolecules, e.g., high acidity/alkalinity, high temperature, or organic surrounding. The multi-step protocol may also suffer from inhomogeneous dispersion of nanoparticles and limited load of the biomolecules. To our knowledge, there are no reports on the convenient and efficient one-pot (one-step) preparation of MPBNCs with biomolecules entrapped at high load/activity for bio-applications.

Thiols and dithiols that can strongly anchor on bulk/nano metal surfaces (e.g. Au) have been widely used to construct various self-assembling monolayers (Love et al., 2005). Dithiols can also polymerize through oxidation of the thiol groups and then S–S linking, and polydithiols have found applications in lithium battery (Shouji et al., 1997; Tatsuma et al., 1997), immunosensing (Fu et al., 2007), and enzyme electrodes (Fu et al., 2008, 2009b). As we are aware, the utilization of polydithiols as efficient matrices for bio-applications is now still an emerging area. The polydithiols-based MPBNCs have not been examined to date, though some other polymers synthesized under more rigorous conditions were used to prepare conventional MPNCs (Burke et al., 2002; Chung et al., 2007; Liu et al., 2008a,b; Wei et al., 2006).

The immobilization of enzyme is the key step in constructing a biosensor (Wilson and Turner, 1992). A variety of techniques have been developed for enzyme immobilization on solid surfaces, such as self-assembly (Chen et al., 2007; Zhao et al., 2007), dip coating (Pang et al., 2009), electrodeposition (Zeng et al., 2009),

* Corresponding author. Tel.: +86 731 88865515; fax: +86 731 88865515.
E-mail address: xieqj@hunnu.edu.cn (Q. Xie).

0956-5663/$ – see front matter © 2009 Elsevier B.V. All rights reserved.
doi:10.1016/j.bios.2009.10.014

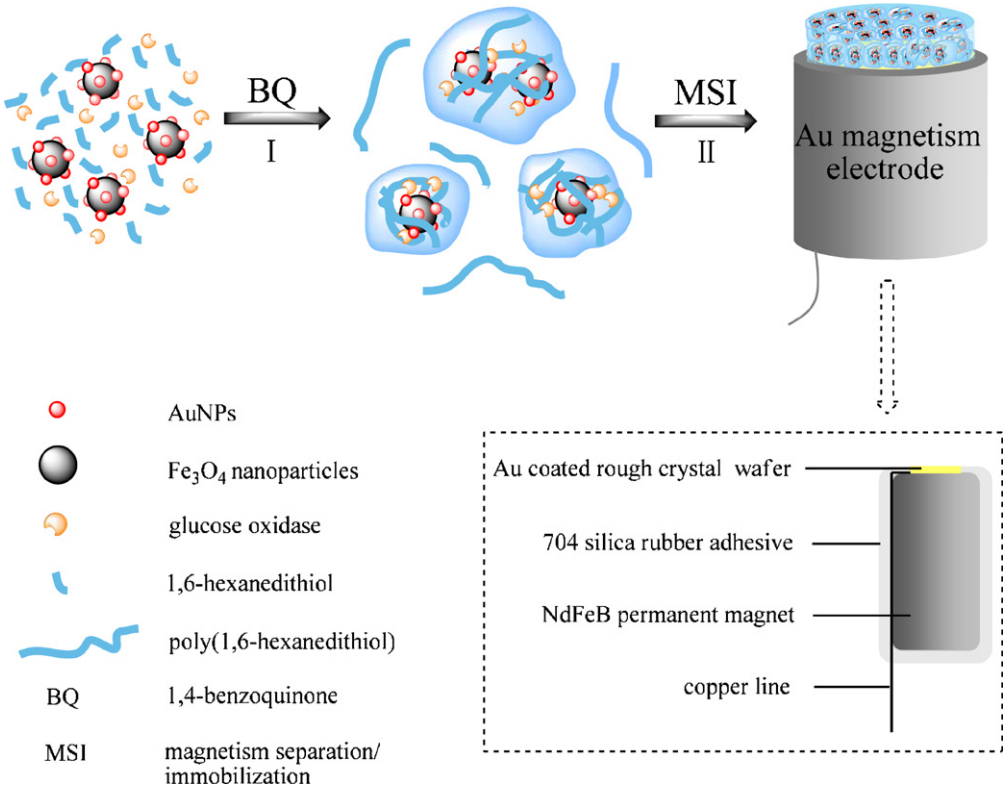

Scheme 1. Schematic illustration of the construction of a Fe_3O_4–Au–PHDT–GOx modified Au magnetism-electrode.

and covalent attachment (Cass et al., 1984; Hrapovic et al., 2004). Very recently, our group reported the protocol of one-pot chemical (or biochemical) preoxidation and electropolymerization of monomers (CPEM or BPEM) in enzyme-containing aqueous suspensions (or solutions) as a universal strategy for high-activity and high-load immobilization of enzymes to construct amperometric biosensors (Fu et al., 2008, 2009b). The CPEM/BPEM protocols combine the advantages of the highly efficient entrapment of enzyme molecules by chemical/biochemical polymerization and the high controllability of electropolymerization for electrode-surface modification. The thus-prepared biosensors perform much better than that using the conventional electropolymerization (CEP) protocol. As a recently emerged protocol for biomolecular immobilization on an electrode, magnetic immobilization is highly selective, efficient, and convenient for electrochemical and biosensing studies, including the magnetic immobilization of leukaemia K562 cells (Jia et al., 2009), enzyme (Elyacoubi et al., 2006; Liu et al., 2005, 2006; Qu et al., 2007; Yu et al., 2006; Zhang et al., 2007), and antibody (Tang et al., 2006). However, the biomolecules are often covalently immobilized on the surfaces of the magnetic particles with limited load, and it is thus interesting to explore new magnetic materials and protocols to immobilize biomolecules at high load and high activity for bio-applications.

Herein, we report on the preparation of MPBNCs-based biosensors using a one-pot chemical oxidation synthesis and magnetism separation/immobilization (COSMSI) protocol for high-performance biosensing of glucose. 1,6-Hexanedithiol (HDT) as a monomer, glucose oxidase (GOx) as a model enzyme, and Fe_3O_4 or Fe_3O_4–Au as model magnetic nanomaterial, are involved. In the COSMSI protocol, to a pH 7.0 phosphate buffer suspension containing ultrasonically dispersed HDT, GOx and magnetic nanoparticles, 1,4-benzoquinone (BQ) is added to oxidize HDT to form poly(HDT) (PHDT) and yield MPBNCs. Some of the prepared MPBNCs are then immobilized on an Au magnetism-electrode through magnetism separation/immobilization, and the thus-prepared biosensor performs better than that using the reported CEP or CPEM protocol.

2. Experimental

2.1. Instrumentation and reagents

All electrochemical experiments were conducted on a CHI660C electrochemical workstation (CH Instrument Co., USA), and a conventional three-electrode electrolytic cell was used. The Au magnetism-electrode (area = 9 mm^2) served as the working electrode, the reference electrode as the KCl-saturated calomel electrode (SCE), and a carbon rod as the counter electrode. All potentials reported in this paper are cited vs. SCE (vs. SCE). A computer-interfaced HP4395A impedance analyzer was employed in the electrochemical quartz crystal microbalance (EQCM) experiments. AT-cut 9 MHz piezoelectric quartz crystals (PQCs) with 12.5-mm wafer diameter (Model JA5, Beijing Chenjing Electronics Co., Ltd., China) were used. The Au electrode with 6.0-mm diameter (key-hole configuration, area = 0.29 ± 0.01 cm^2) on one side of the PQC was exposed to the solution and served as the working electrode (Au_{EQCM}), while that on the other side faced air. Transmission electron microscopy (TEM) pictures were collected on a JEOL-1230 microscope. Scanning electron microscopy (SEM) pictures were collected on a JEM-6700F field emission scanning electron microscope. Ultraviolet–visible (UV–vis) spectra were recorded on a Shimadzu UV-2450 UV–vis spectrophotometer.

GOx (EC 1.1.3.4; type II from *Aspergillus niger*, activity ≈ 150 kU g^{-1}) was purchased from Sigma. HDT was a product of Alfa Aesar. Glucose was obtained from Shanghai Chemicals Station. A pH 7.0 phosphate buffer solution (PBS), 0.1 M KH_2PO_4–K_2HPO_4 + 0.1 M K_2SO_4, was used. All other chemicals were of analytical grade or better quality, and used as received. Milli-Q

ultrapure water (Millipore, ≥18 MΩ cm) was used throughout. All experiments were performed at room temperature around 20 °C.

2.2. Preparation and characterization of MPBNCs

Fe_3O_4 nanoparticles were prepared by the chemical coprecipitation method with a slight modification (Pang et al., 2007). Nitrogen gas was used in the whole process. $FeCl_3{\cdot}6H_2O$ (2.7 g) and $FeCl_2{\cdot}4H_2O$ (1.0 g) were ultrasonically dissolved in 100 mL of 1.2 mM aqueous HCl. 1.25 M aqueous NaOH (150 mL) was then added under vigorous stirring, and a black precipitate formed immediately. After vigorous stirring for 30 min, the precipitate was magnetically separated and washed thoroughly with water till the supernatant liquor reached neutrality (pH ~ 7). The final precipitate was dispersed in 250 mL of water, and then directly used to prepare Fe_3O_4–Au nanocomposites as follows.

4.0 mL of 4% $HAuCl_4$ was added dropwise to 250 mL of the Fe_3O_4 suspension under vigorous stirring, then 20 mL of 0.8 M $NH_2OH{\cdot}HCl$ was added, and the solution color immediately turned from black to deep red. After vigorous stirring for 30 min, another 4.0 mL of 4% $HAuCl_4$ was added to the mixture, followed by vigorous stirring for another 1 h. The yielded deep red precipitate was magnetically separated and washed with water four times to remove any nonmagnetic particles, then it was dispersed into 25 mL of water and stored at 4 °C in a refrigerator. The final concentration of Fe_3O_4–Au was 26.7 mg mL^{-1}, as measured by vacuum drying a certain volume of Fe_3O_4–Au nanocomposites and weighing the product.

The MPBNCs were prepared as illustrated in Scheme 1 (from I to II). 0.401 mg mL^{-1} Fe_3O_4–Au and 0.375 mg mL^{-1} GOx (final concentration for each) were added to 1.0 mL PBS containing 0.25 mg mL^{-1} ultrasonically dispersed HDT under stirring. Then, 33 μL of 0.05 M BQ was added to oxidize and polymerize HDT, and the mixture was slowly stirred for 5 min to form Fe_3O_4–Au–PHDT–GOx MPBNCs with plenty of GOx molecules entrapped, then magnetically separated for future use. The final concentration of Fe_3O_4–Au–PHDT–GOx MPBNCs was 0.850 mg mL^{-1}, as measured similarly by vacuum drying.

We have estimated the enzymatic specific activity (ESA) of the native GOx dissolved in PBS and the GOx in MPBNCs (after magnetic separation and dispersion in PBS, see Supplemental Data for details). The ESA is defined as the ratio of molar quantity of enzymatically generated H_2O_2 in (mol in 60 s to the mass of enzyme in g (Fu et al., 2009a, 2008). As listed in Table 1S, ca. 83% of initial GOx has been captured by the MPBNCs, and the GOx in the MPBNCs keeps as high as 70% activity of the native enzyme, indicating the immobilization of GOx in the MPBNCs at high load/activity.

2.3. Fabrication and characterization of the enzyme electrodes

To clean the Au electrode surface, a drop of fresh prepared concentrated $H_2SO_4 + H_2O_2$ (3:1, v/v) was cast on the electrode surface. After kept for 15 s, the electrode was rinsed thoroughly with water and dried with a stream of pure nitrogen. The treatment was repeated three times. Prior to electrochemical experiments, the Au electrode was subject to continuous potential cycling (0–1.5 V, 30 mV s^{-1}) in 0.20 M aqueous $HClO_4$, until the cyclic voltammogram became reproducible.

The Au magnetism-electrode was fabricated as follows. As shown in Scheme 1, a gold thin film was coated on the surface of a rough quartz crystal wafer using a KYKY SBC-12 ion coater (Zhongkekeyi, Beijing). The Au coated side served as the working electrode, while the other side of the quartz wafer was adhered to one terminal of a piece of NdFeB permanent magnet (8 mm diameter and 10 mm height). A silica rubber adhesive (Nanda 704, China) was used to seal the magnet and the crystal wafer, leaving 9.0 mm^2 geometrical surface area of the Au electrode exposed.

200 μL of 0.850 mg mL^{-1} Fe_3O_4–Au–PHDT–GOx aqueous suspension was cast onto the bare Au magnetism-electrode, the solid MPBNCs were magnetically attracted down to the electrode surface immediately from the suspension, and the supernatant liquor was removed using a pipette. The modified Au magnetism-electrode was air-dried for future use.

In the CPEM case, 1.0 mg mL^{-1} GOx (final concentration) was added to an ultrasonically dispersed aqueous suspension of 0.5 mg mL^{-1} HDT in 1.0 mL PBS under stirring, then 60 μL of 0.05 M BQ was slowly added. The mixture was slowly stirred for 5 min to form PHDT–GOx composites, then the codeposition of some PHDT–GOx composites during potentiostatic electropolymerization of excess HDT at 1.3 V was performed to achieve a 6.0-kHz film on Au_{EQCM} (PHDT–GOx–BQ/Au_{EQCM}), as monitored by the EQCM technique (Fig. 1S). The electrode was then thoroughly rinsed with water to remove physically adsorbed species.

In the CEP case, 1.0 mg mL^{-1} GOx (final concentration) was added to 1.0 mL of PBS suspension containing 0.5 mg mL^{-1} HDT, followed by 1.3 V potentiostatic electropolymerization to grow a 2.0-kHz polymer on Au_{EQCM} (PHDT–GOx/Au_{EQCM}), simultaneously with EQCM monitoring (Fig. 1S), then the resulted electrode was water-rinsed thoroughly.

When not in use, the prepared enzyme electrodes were stored in pH 7.0 PBS at 4 °C (refrigerator).

2.4. Amperometric measurements

The measurements of the prepared enzyme electrodes were carried out at 0.7 V in stirred pH 7.0 PBS (Fu et al., 2008, 2009b), and the response current was marked with the change value between the steady-state current after adding a substrate and the initial background current without the substrate.

3. Results and discussion

3.1. Characterization of the MPBNCs and optimization of biosensing conditions

The water-soluble Fe_3O_4–Au nanocomposites can be prepared by reduction of Au^{3+} onto the Fe_3O_4-seed surfaces using a sodium citrate or hydroxylamine seeding procedure (Lu et al., 2006; Lyon et al., 2004; Pang et al., 2007; Pham et al., 2008). The sodium citrate seeding method suffered from the drawbacks of the requirement for a boiling H_2O and the possibility of the new particle nucleation in solution simultaneously with the seed-surface nucleation during Au^{3+} reduction (Brown et al., 2000). However, the hydroxylamine seeding could be carried out at room temperature, with a solution nucleation rate constant of zero and a surface nucleation rate constant significantly greater than zero at room temperature (Brown et al., 2000). Herein, we synthesized the Fe_3O_4–Au nanocomposites by Au^{3+} reduction onto the Fe_3O_4 surfaces using the modified hydroxylamine seeding procedure as above.

The UV–vis spectra of thus-prepared Fe_3O_4, Fe_3O_4–Au, and Fe_3O_4–Au–PHDT–GOx are shown in Fig. 1. No significant absorption peak was observed for pure Fe_3O_4, while the absorption peaks occurred at 540 nm for Fe_3O_4–Au, due to the plasmon absorption of nanosized Au in Fe_3O_4–Au. Note that we failed to synthesize pure Au nanoparticles via the hydroxylamine seeding procedure, as reported previously (Lu et al., 2006; Lyon et al., 2004; Pang et al., 2007; Pham et al., 2008). Generally, the surface plasmon of pure Au nanoparticles prepared by the sodium citrate seeding procedure causes an absorption peak around 520 nm (Daniel and Astruc, 2004). The red-shift of the surface plasmon spectra observed here (540 nm vs. 520 nm) may result from the increased size of Au nanoparticles and deficient electron population on Au for the

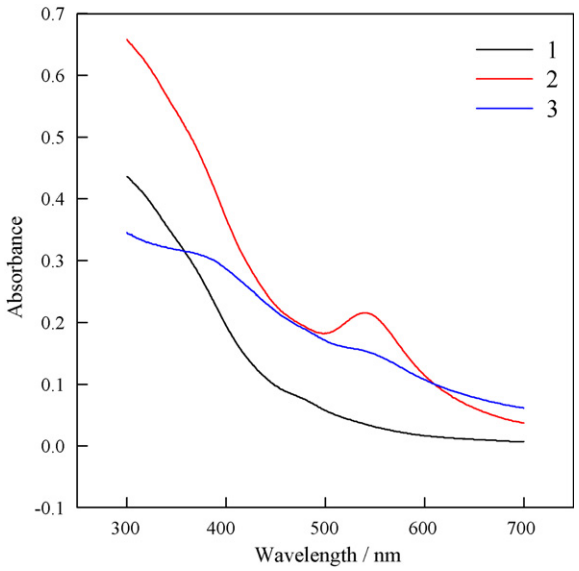

Fig. 1. UV–vis spectra of Fe_3O_4 (1) nanoparticles as well as Fe_3O_4–Au (2) and Fe_3O_4–Au–PHDT–GOx (3) nanocomposites.

interfacial communication between Au and Fe_3O_4 nanoparticles in Fe_3O_4–Au (Daniel and Astruc, 2004; Pang et al., 2007; Yu et al., 2005). For the MPBNCs, an obviously suppressed Au absorption peak was observed, since the added PHDT–GOx and the formed covalent Au–S bonds should decrease the number of electrons involved in the surface plasmon.

The magnetic effects on as-prepared Fe_3O_4 nanoparticles, Fe_3O_4–Au nanocomposites, the diluted HCl-treated Fe_3O_4–Au nanocomposites, and MPBNCs were studied (Fig. 2S). The Fe_3O_4 nanoparticles presented black color, while the Fe_3O_4–Au, the diluted HCl-treated Fe_3O_4–Au nanocomposites, and MPBNCs presented deep red color due to the existence of nanosized Au. Upon the application of a magnetic field by a magnet, all of the nanoparticles/nanocomposites aggregated immediately, and the supernatant liquors became almost colorless, indicating that the Au and PHDT–GOx moieties were robustly tethered to Fe_3O_4, and they perfectly co-aggregated with Fe_3O_4 of excellent superparamagnetic property in the magnetic field. Also, the HCl-treated Fe_3O_4–Au nanocomposites exhibited a magnetic behavior, proving the entrapment of Fe_3O_4 in the Fe_3O_4–Au nanoparticles.

TEM pictures of the prepared Fe_3O_4, Fe_3O_4–Au, and Fe_3O_4–Au–PHDT–GOx are shown in Fig. 2. The grayish colored Fe_3O_4 are observed with uniform dispersion in ~10 nm diameter on average (picture (a)). The prepared Fe_3O_4–Au nanocomposites appear as dark colored particles of ~50 nm diameter with coexisting Fe_3O_4 nanoparticles (picture (b)). Increasing the quantity ratio of $HAuCl_4$ to Fe_3O_4 can increase the number of dark colored nanoparticles, but the uncovered Fe_3O_4 nanoparticles are still seen (Fig. 3S). According to the previous report (Lyon et al., 2004), the growth of AuNPs should take place preferably on the Fe_3O_4-seed surfaces, since hydroxylamine triggers surface catalyzed reduction of Au^{3+} rather than solution-state Au nucleation, implying here that the Au is coated on the surfaces of Fe_3O_4 nanoparticles. Hence, the dark colored nanoparticles should be the Au coated Fe_3O_4 or their aggregates. In comparison with the clear silhouette of Fe_3O_4–Au (picture (b)), the uninterrupted gray-colored surrounding of Fe_3O_4–Au and Fe_3O_4 particles is assumed to be the PHDT–GOx shell (picture (c)).

SEM pictures of Au-supported Fe_3O_4–Au and MPBNCs, as well as the electropolymerized PHDT–GOx–BQ film are also shown (Fig. 2). Both Fe_3O_4–Au and Fe_3O_4–Au–PHDT–GOx are uniformly dispersed on Au (pictures (d) and (e)), while a block and more compact PHDT–GOx–BQ film similar to our previous report (Fu et al., 2008, 2009b) is seen (picture (f)).

In order to maximize the detection sensitivity of the MPBNCs-based enzyme electrodes, we optimized various conditions, including the concentrations of HDT, GOx, BQ and Fe_3O_4–Au, as well as the coating amount of Fe_3O_4–Au–PHDT–GOx composites, via changing the examined condition while the others were fixed. As shown in Fig. 4S, the response current to 2.00 mM glucose increased with the increase of HDT concentration from 0.1 to 0.25 mg mL^{-1}, and beyond this range the response current decreased, thus 0.25 mg mL^{-1} HDT was selected. The response current became saturated at BQ concentrations over 1.65 mM (1:1 molar ratio of BQ to HDT), thus 1.65 mM was selected. The optimized GOx concentration with a maximum response is 0.375 mg mL^{-1}. The higher

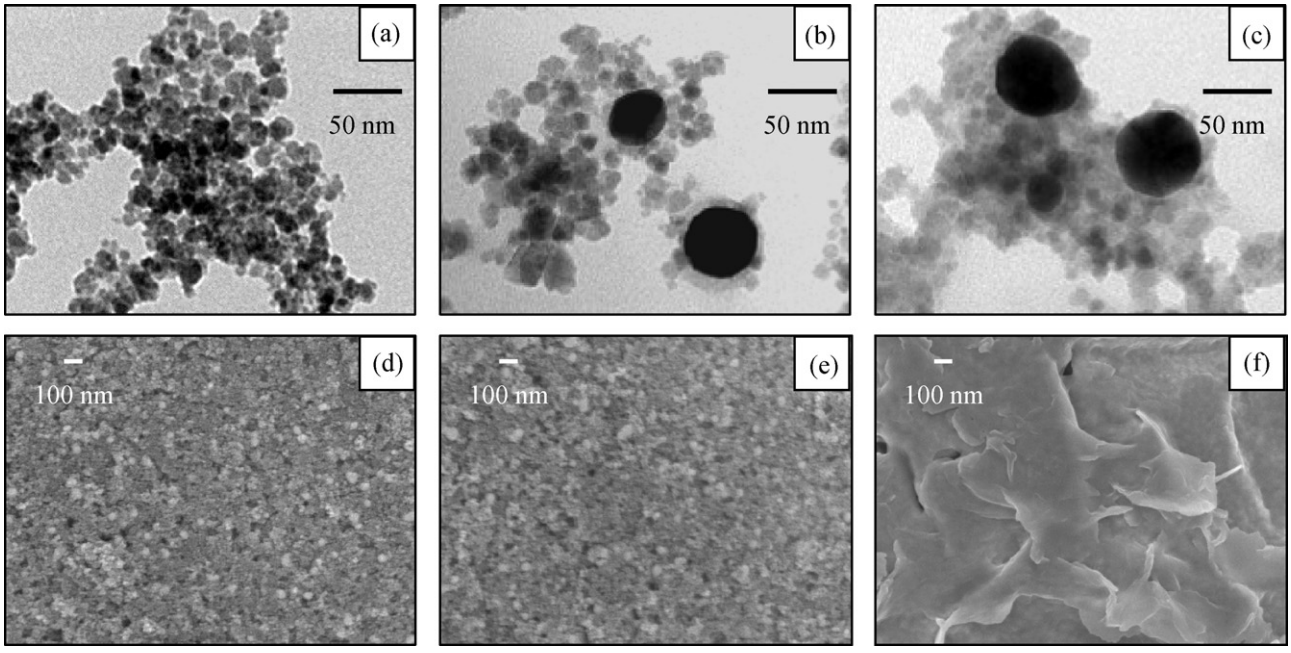

Fig. 2. TEM pictures of Fe_3O_4 (a), Fe_3O_4–Au (b) and Fe_3O_4–Au–PHDT–GOx (c) as well as SEM pictures of Fe_3O_4–Au (d), Fe_3O_4–Au–PHDT–GOx (e), and PHDT–GOx–BQ (f).

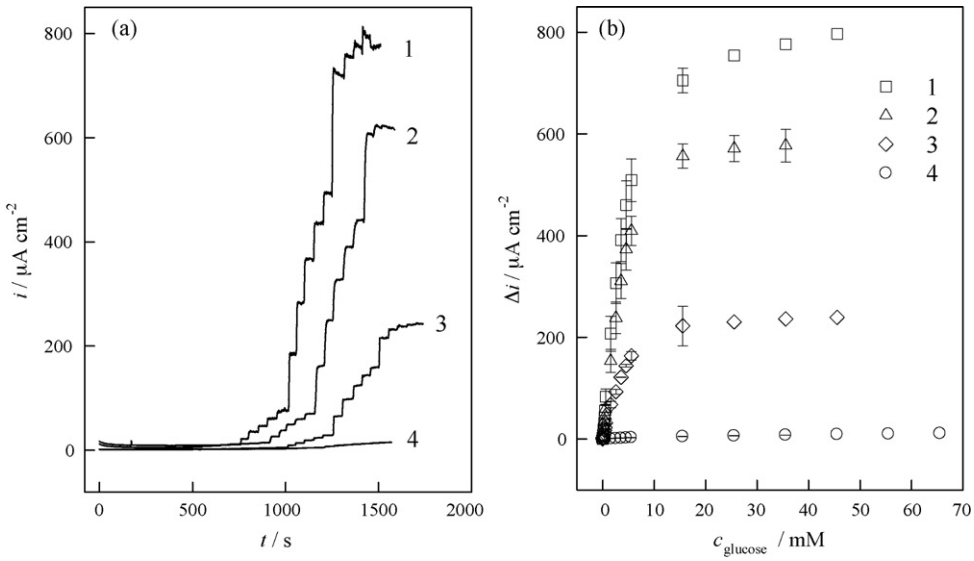

Fig. 3. Chronoamperometric responses to successive additions of glucose (a) and the calibration curves (b) on Fe_3O_4–Au–PHDT–GOx/Au (1), Fe_3O_4–PHDT–GOx/Au (2), PHDT–GOx–BQ/Au (3), and PHDT–GOx/Au (4) at 0.7 V vs. SCE in pH 7.0 PBS. The enzyme electrodes were fabricated under optimized conditions.

concentration of Fe_3O_4–Au can form thinner PHDT shell with little GOx entrapped, while a lower concentration of Fe_3O_4–Au may cause a thicker PHDT shell against the mass transfer and the production of some free-standing PHDT–GOx particles without inner Fe_3O_4–Au (waste of GOx during magnetism separation). The optimized concentration of Fe_3O_4–Au is 0.401 mg mL^{-1}. The optimized volume of the 0.850 mg mL^{-1} MPBNCs aqueous suspension cast on the bare Au magnetism-electrode is 200 μL (170 μg MPBNCs).

3.2. Biosensing performance

Under the optimized conditions, the performance of the prepared MPBNCs electrodes was examined. The amperometric responses and calibration curves are shown in Fig. 3, and the values of sensitivity, linear detection range (LDR), and limit of detection (LOD, S/N = 3) are listed in Table 1.

The biosensors prepared by the COSMSI protocol (Fe_3O_4–Au–PHDT–GOx/Au and Fe_3O_4–PHDT–GOx/Au) present notably increased sensitivities, being 2.7 and 2.2 folds that by the CPEM protocol (PHDT–GOx–BQ/Au), and 207 and 170 folds that by the CEP protocol (PHDT–GOx/Au), respectively. Also, these sensitivities are superior to those for most of other glucose biosensors prepared by other protocols (Chen et al., 2007; Hrapovic et al., 2004; Kaushika et al., 2008; Liu et al., 2008b; Pang et al., 2009; Zeng et al., 2009; Zhao et al., 2007). The COSMSI-based biosensors show sub-μM LOD, and excellent anti-interferent ability against ascorbic acid (AA) and uric acid (UA), as shown in Fig. 5S. In contrast, the Fe_3O_4–Au–GOx based electrode presents low sensitivity and poor anti-interferent ability (Fig. 6S). We found that the PHDT film is responsible for the anti-interferent ability, which can maintain the response to electrooxidation of H_2O_2, but largely inhibit the electrooxidation of AA and UA. As shown in Table 2S (potentiostatic responses at 0.7 V vs. SCE), in comparison with the bare Au electrode, the PHDT–GOx–BQ and MPBNCs modified Au electrodes keep ~80% and ~58% responses for H_2O_2, but less than 10% for AA and UA, respectively. Cyclic voltammetric experiments also generated similar permselectivity results (not shown). The thick and nonconducting PHDT film acts here as a diffusional barrier to the electroactive substances. The size of the electroactive substance is an important parameter to affect its permeation rate through the film and the electrode response. The smaller H_2O_2 molecule diffuses more easily through the film than the larger UA and AA molecules, making the oxidation current of H_2O_2 less inhibited as observed. Similar findings have been reported for other nonconducting polymers such as poly(substituted naphthalene) (Murphy, 1998), poly(phenylenediamine) (Dai et al., 2006) and poly(*o*-aminophenol) (Pan et al., 2005).

Table 1
Construction and performance of several enzyme electrodes.

Protocol	Enzyme electrodes	Sensitivity/μA cm^{-2} mM^{-1}	LDR/μM	LOD/μM	References
CEP	PHDT–GOx/Au	0.53	100–5500 (r^2 = 0.9977)	31	This work
CPEM	PHDT–GOx–BQ/Au	41	2.0–1600 (r^2 = 0.9940)	0.51	This work
COSMSI	Fe_3O_4–PHDT–GOx/Au	90	2.0–1600 (r^2 = 0.9977)	0.66	This work
COSMSI	Fe_3O_4–Au–PHDT–GOx/Au	110	2.0–2600 (r^2 = 0.9989)	0.33	This work
Self-assembling	HFBI–GOx/Pt	4.21	500–20,000	90	(Zhao et al., 2007)
Dip coating	GOx/Pt/CNT/TiO_2	0.24	6–1500	5.7	(Pang et al., 2009)
Layer-by-layer assembling	$(PDDA/GOx)_5$/Nafion/PtC/GC	9.55	50–7000	20	(Chen et al., 2007)
Electrodeposition	CS–IL–GOx/nano–Au	14.3	3.0–9000	1.5	(Zeng et al., 2009)
Crosslinking	CNT–Pt_{nano}–GOx/GC	30	0.5–5000	0.5	(Hrapovic et al., 2004)
Electrochemical doping/magnetic immobilization	PA–Fe_3O_4–CNT–GOx/graphite–epoxy	82.6			(Liu et al., 2008b)
Electrostatic interaction	GOx/CH–Fe_3O_4/ITO	9.3	500–22,000	500	(Kaushika et al., 2008)

LDR = linear detection range; LOD = limit of detection.

The storage stability of the prepared enzyme electrodes was investigated. The time periods for the enzyme electrodes retaining 80% of their initial responses were found to be 1, 4, 12, and 10 weeks for PHDT–GOx/Au, PHDT–GOx–BQ/Au, Fe_3O_4–Au–PHDT–GOx/Au and Fe_3O_4–PHDT–GOx/Au, respectively, indicating highly efficient immobilization of GOx in the later two films.

It should be noted the magnet plays a key role in the biosensing experiments. After the enzyme electrode without the magnet was water-rinsed thoroughly, the MPBNCs film almost fell off, leaving a firmly attached thin surface layer on the electrode due to the Au–S binding, and the biosensing response was decreased by 90% of its initial one.

The present COSMSI protocol is indeed promising for constructing high-performance biosensors, being mainly due to the in situ chemical oxidation synthesis with high-load and high-activity enzyme entrapped in the MPBNCs and the magnetic separation/immobilization method with the MPBNCs firmly immobilized on the electrode. The metal–S bonding of –SH with AuNPs and Fe_3O_4 can efficiently stabilize the MPBNCs, the highly biocompatible Fe_3O_4 and AuNPs provide the entrapped enzyme molecules with a friendly microenvironment to efficiently prevent them from denaturalization (Wang et al., 2008), and the AuNPs can increase the film conductivity, leading to the improvement of sensitivity and stability of the Fe_3O_4–Au–PHDT–GOx biosensor vs. the Fe_3O_4–PHDT–GOx one.

4. Conclusions

In summary, the addition of an oxidant BQ to an aqueous HDT suspension containing GOx and Fe_3O_4–Au has yielded new Fe_3O_4–Au–PHDT–GOx MPBNCs with GOx entrapped at high load/activity. The Fe_3O_4–Au–PHDT–GOx has been conveniently separated through a magnet and efficiently immobilized on an Au magnetism-electrode for glucose biosensing, and the biosensing performance is obviously better than that of the biosensors based on other typical protocols reported. The proposed chemical oxidation synthesis and magnetism separation/immobilization protocol may be interesting in many fields, such as biosensing, biocatalysis, biofuel cells and bioaffinity separation.

Acknowledgements

This work was supported by the National Science Foundation of China (20675029, 90713018, 20335020), the State Special Scientific Project on Water Treatment (2009ZX07212-001-06), the Foundation of the Ministry of Education of China and of Hunan Provincial Educational Department (05K009, 05A036), and the State Key Laboratory of Electroanalytical Chemistry. Zou and Fu contributed equally to this work.

Appendix A. Supplementary data

Supplementary data associated with this article can be found, in the online version, at doi:10.1016/j.bios.2009.10.014.

References

Altintas, E.B., Tuezmen, N., Candan, N., Denizli, A., 2007. J. Chromatogr. B 853, 105–113.
Bayramoglu, G., Yilmaz, M., Senel, A.U., Arica, M.Y., 2008. Biochem. Eng. J. 40, 262–274.
Brown, K.R., Walter, D.G., Natan, M.J., 2000. Chem. Mater. 12, 306–313.
Burke, N.A.D., Stover, H.D.H., Dawson, F.P., 2002. Chem. Mater. 14, 4752–4761.
Cao, X.D., Li, C.M., Bao, H.F., Bao, Q.L., Dong, H., 2007. Chem. Mater. 19, 3773–3779.
Cass, A.E.G., Davis, G., Francis, G.D., Hill, H.A.O., Aston, W.J., Higgins, I.J., Plotkin, E.V., Scott, L.D.L., Turner, A.P.F., 1984. Anal. Chem. 56, 667–671.
Chen, X., Yan, X., Khor, K.A., Tay, B.K., 2007. Biosens. Bioelectron. 22, 3256–3260.
Chung, T.H., Pan, H.C., Lee, W.C., 2007. J. Magn. Magn. Mater. 311, 36–40.
Dai, Y.Q., Zhou, D.M., Shiu, K.K., 2006. Electrochim. Acta 52, 297–303.
Dang, Z.M., Lin, Y.Q., Xu, H.P., Shi, C.Y., Li, S.T., Bai, J.B., 2008. Adv. Funct. Mater. 18, 1509–1517.
Daniel, M.C., Astruc, D., 2004. Chem. Rev. 104, 293–346.
Elyacoubi, A., Zayed, S.I.M., Blankert, B., Kauffmann, J.M., 2006. Electroanalysis 18, 345–350.
Fu, Y., Li, P., Xie, Q., Xu, X., Lei, L., Chen, C., Zou, C., Deng, W., Yao, S., 2009a. Adv. Funct. Mater. 19, 1784–1791.
Fu, Y.C., Chen, C., Xie, Q.J., Xu, X.H., Zou, C., Zhou, Q.M., Tan, L., Tang, H., Zhang, Y.Y., Yao, S.Z., 2008. Anal. Chem. 80, 5829–5838.
Fu, Y.C., Xie, Q.J., Jia, X.E., Xu, X.H., Meng, W.H., Yao, S.Z., 2007. J. Electroanal. Chem. 603, 96–106.
Fu, Y.C., Zou, C., Xie, Q.J., Xu, X.H., Chen, C., Deng, W.F., Yao, S.Z., 2009b. J. Phys. Chem. B 113, 1332–1340.
Granot, E., Katz, E., Basnar, B., Willner, I., 2005. Chem. Mater. 17, 4600–4609.
Gu, H., Xu, K., Xu, C., Xu, B., 2006. Chem. Commun., 941–949.
Hong, J., Xu, D., Gong, P., Yu, J., Ma, H., Yao, S., 2008. Micropor. Mesopor. Mater. 109, 470–477.
Hrapovic, S., Liu, Y., Male, K.B., Luong, J.H.T., 2004. Anal. Chem. 76, 1083–1088.
Huang, J., Han, B., Yue, W., Yan, H., 2007. J. Mater. Chem. 17, 3812–3818.
Huang, J.S., Li, X.T., Zheng, Y.H., Zhang, Y., Zhao, R.Y., Gao, X.C., Yan, H.S., 2008. Macromol. Biosci. 8, 508–515.
Jia, X., Tan, L., Zhou, Y., Jiang, X., Xie, Q., Tang, H., Yao, S., 2009. Electrochem. Commun. 11, 141–144.
Kaushika, A., Khan, R., Solanki, P.R., Pandey, P., Alam, J., Ahmad, S., Malhotra, B.D., 2008. Biosens. Bioelectron. 24, 676–683.
Krizova, J., Spanova, A., Rittich, B., Horak, D., 2005. J. Chromatogr. A 1064, 247–253.
Lei, Z.L., Ren, N., Li, Y.L., Li, N., Mu, B., 2009. J. Agric. Food Chem. 57, 1544–1549.
Liu, H., Guo, J., Jin, L., Yang, W., Wang, C., 2008a. J. Phys. Chem. B 112, 3315–3321.
Liu, Z., Liu, Y., Yang, H., Yang, Y., Shen, G., Yu, R., 2005. Anal. Chim. Acta 533, 3–9.
Liu, Z., Liu, Y., Yang, H., Yang, Y., Shen, G., Yu, R., 2006. Biotechnol. Lett. 28, 559–565.
Liu, Z., Wang, J., Xie, D.H., Chen, G., 2008b. Small 4, 462–466.
Love, J.C., Estroff, L.A., Kriebel, J.K., Nuzzo, R.G., Whitesides, G.M., 2005. Chem. Rev. 105, 1103–1170.
Lu, Q.H., Yao, K.L., Xi, D., Liu, Z.L., Luo, X.P., Ning, Q., 2006. J. Magn. Magn. Mater. 301, 44–49.
Lyon, J.L., Fleming, D.A., Stone, M.B., Schiffer, P., Williams, M.E., 2004. Nano Lett. 4, 719–723.
Morais, J., Azevedo, R.B., Silva, L.P., Lacava, Z.G.M., Bao, S.N., Silva, O., Pelegrini, F., Gansau, C., Buske, N., Safarik, I., Safarikova, M., Morais, P.C., 2004. J. Magn. Magn. Mater. 272, 2400–2401.
Murphy, L.J., 1998. Anal. Chem. 70, 2928–2935.
O'Mullane, A.P., Dale, S.E., Macpherson, J.V., Unwin, P.R., 2004. Chem. Commun., 1606–1607.
Olsvik, O., Popovic, T., Skjerve, E., Cudjoe, K.S., Hornes, E., Ugelstad, J., Uhlen, M., 1994. Clini. Microbiol. Rev. 7, 43–54.
Pan, D., Chen, J., Yao, S., Nie, L., Xia, J., Tao, W., 2005. Sens. Actuators B 104, 68–74.
Pang, L.L., Li, J.S., Jiang, J.H., Le, Y., Shen, G.L., Yu, R.Q., 2007. Sens. Actuators B 127, 311–316.
Pang, X., He, D., Luo, S., Cai, Q., 2009. Sens. Actuators B 137, 134–138.
Pham, T.T.H., Cao, C., Sim, S.J., 2008. J. Magn. Magn. Mater. 320, 2049–2055.
Qu, S., Wang, J., Kong, J., Yang, P., Chen, G., 2007. Talanta 71, 1096–1102.
Schoepf, U., Marecos, E.M., Melder, R.J., Jain, R.K., Weissleder, R., 1998. Biotechniques 24, 642–651.
Shen, Y., Lin, Y.H., Nan, C.W., 2007. Adv. Funct. Mater. 17, 2405–2410.
Shouji, E., Yokoyama, Y., Pope, J.M., Oyama, N., Buttry, D.A., 1997. J. Phys. Chem. B 101, 2861–2866.
Tang, D., Yuan, R., Chai, Y., 2006. J. Phys. Chem. B 110, 11640–11646.
Tang, D., Yuan, R., Chai, Y., 2008. Anal. Chem. 80, 1582–1588.
Tatsuma, T., Yokoyama, Y., Buttry, D.A., Oyama, N., 1997. J. Phys. Chem. B 101, 7556–7562.
Ventura, M.J., Gu, M., 2008. Adv. Mater. 20, 1329–1332.
Wang, S., Tan, Y., Zhao, D., Liu, G., 2008. Biosens. Bioelectron. 23, 1781–1787.
Wei, H., Wang, E., 2008. Anal. Chem. 80, 2250–2254.
Wei, S.S., Zhu, Y.F., Zhang, Y., Xu, J.R., 2006. React. Funct. Polym. 66, 1272–1277.
Wilson, R., Turner, A.P.F., 1992. Biosens. Bioelectron. 7, 165–185.
Yang, H.H., Zhang, S.Q., Chen, X.L., Zhuang, Z.X., Xu, J.G., Wang, X.R., 2004. Anal. Chem. 76, 1316–1321.
Yu, D., Renedo, O.D., Blankert, B., Sima, V., Sandulescu, R., Arcos, J., Kauffmann, J.M., 2006. Electroanalysis 18, 1637–1642.
Yu, H., Chen, M., Rice, P.M., Wang, S.X., White, R.L., Sun, S., 2005. Nano Lett. 5, 379–382.
Zeng, X., Li, X., Xing, L., Liu, X., Luo, S., Wei, W., Kong, B., Li, Y., 2009. Biosens. Bioelectron. 24, 2898–2903.
Zhang, H., Zhong, X., Xu, J.J., Chen, H.Y., 2008. Langmuir 24, 13748–13752.
Zhang, Y., Zeng, G.M., Tang, L., Huang, D.L., Jiang, X.Y., Chen, Y.N., 2007. Biosens. Bioelectron. 22, 2121–2126.
Zhao, Z., Qiao, M., Yin, F., 2007. Biosens. Bioelectron. 22, 3021–3027.